

Progress in Nuclear Energy  
Manuscript Draft

Manuscript Number: PNUCENE-D-16-00533

Title: Steady RANS Methodology for Calculating Pressure Drop in an In-Line Molten Salt Compact Crossflow Heat Exchanger

Article Type: Research Paper

Keywords: Computational Fluid Dynamics; Steady RANS; Cross flow; Tube Bank; Heat Exchangers

## **Highlights**

### **Highlight:**

- Flow behavior in a compact tube bank using steady RANS was investigated.
  - Boundary conditions in the spanwise direction that effect the desired parameters were determined.
  - A minimum size of the domain was determined.
  - A feasible turbulence model was determined for a steady framework.
- 

1  
2  
3  
4 **Title:** Steady RANS Methodology for Calculating Pressure Drop in an In-Line Molten Salt  
5 Compact Crossflow Heat Exchanger  
6  
7  
8

9 **Authors:**

10 Lane B. Carasik<sup>1</sup>, Dillon R. Shaver<sup>2</sup>, Jonah B. Haefner<sup>1</sup>, Yassin A. Hassan<sup>1</sup>  
11  
12

13 <sup>1</sup>Department of Nuclear Engineering, Texas A&M University, 3133 TAMU, College Station, TX,  
14 77845

15 <sup>2</sup>NE Division, Argonne National Laboratories, Argonne, IL 60439

16 **Abstract:**

17 The development of molten salt reactors requires the use of advanced design tools for the primary  
18 heat exchanger design. Due to geometric and flow characteristics, compact (pitch to diameter  
19 ratios equal to or less than 1.25) heat exchangers with a crossflow flow arrangement can become  
20 desirable for these reactors. Unfortunately, the available experimental data is limited for compact  
21 tube bundles in crossflow. Computational Fluid Dynamics can be used to alleviate the lack of  
22 experimental data. Previous computational efforts have been primarily focused on large P/D ratios  
23 using unsteady Reynolds averaged Navier-Stokes and Large Eddy Simulation frameworks. These  
24 approaches are useful, but have large computational requirements which make design studies using  
25 them impractical. In an effort to provide a starting point for future design work, a CFD study  
26 focused on implementing steady RANS was conducted. The study was performed for an in-line  
27 tube bank geometry with FLiBe (LiF-BeF<sub>2</sub>), a frequently selected molten salt, as the working  
28 fluid. Based on the estimated pressure drops and the pressure and velocity distributions in the  
29 domain, an appropriate meshing strategy was determined and presented. Periodic boundaries in  
30 the spanwise direction transverse flow were determined to be an appropriate boundary condition.  
31 The domain size was investigated and a minimum of 2-flow channels for a domain is  
32 recommended. Lastly, the standard low Re  $\kappa$ - $\epsilon$  (Lien) turbulence model was found to be the most  
33 appropriate for steady RANS of this case.

34 **Keywords:**

35 Computational Fluid Dynamics, Steady RANS, Crossflow, Tube Bank, Heat Exchangers

36 **Highlight:**

37 -Flow behavior in a compact tube bank using steady RANS was investigated.

38 -Boundary conditions in the spanwise direction that effect the desired parameters were determined

39 -A minimum size of the domain was determined.

40 -A feasible turbulence model was determined for a steady framework.

1  
2  
3  
4     1     Introduction:

5  
6     Advanced reactor designs are garnering interest for usage in future energy markets. The majority  
7     of these advanced reactors are designed with significant improvements over operating light water  
8     reactors (LWRs). One notable improvement is the higher operating temperatures (~500-900 C)  
9     than currently operating reactors (~250-325 C). This allows for higher thermal efficiencies for  
10    power conversion as compared to the currently operating fleet of nuclear and fossil-fueled plants.  
11  
12

13     Nuclear power plants are usually operated with both “primary” and “secondary” loops connected  
14    by a heat exchanger. In addition to this heat exchanger, the primary side contains the reactor and  
15    coolant pumps, whereas the secondary side contains pumps and the standard equipment for power  
16    conversion seen in thermal power plants. One particularly promising class of advanced reactors  
17    are molten salt reactors (MSRs) which are unique in that the fuel design can be either solid and  
18    separated from the coolant or dissolved directly in the coolant. MSRs have two radically different  
19    types of primary loop side designs. The first is the more traditional loop-type, featuring solid fuel  
20    and a liquid coolant circulated via piping. The second is a pool-type which contains the  
21    components in one pressure vessel filled with coolant. For pool-type MSRs, the design of the  
22    primary heat exchangers (PHXs) can be radically different from the more traditional designs  
23    featured in loop-type MSRs. This is important for the operations and heat transfer from the primary  
24    to secondary loops and represents a significant challenge in efficient reactor design.

25  
26     Due to the unique challenges associated with pool-type MSRs, the design of the PHXs that connect  
27    the primary and secondary loops can become complicated. These complications have led to  
28    investigations of different heat exchanger types to reduce the inventory of coolant and maximize  
29    the heat transfer of PHXs. Different heat exchangers types investigated are discussed by  
30    Sabharwall (Sabharwall et al., 2012) and include shell and tube, printed circuit, helical coil, and  
31    other types. Shell and tube heat exchangers are a very common used type which can be used in  
32    parallel, counter-flow, and crossflow fluid arrangements. The crossflow arrangement has had  
33    limited applications in nuclear power due to a variety of factors such as significant fluid structure  
34    interactions and limited experimental and computational studies. Despite this, crossflow heat  
35    exchangers have an advantage in that they can allow for a more open geometry on the shell side  
36    which helps reduce the salt inventory without significantly reducing heat transfer.

37  
38     The PHX used in the design of the Small modular Advanced High Temperature Reactor  
39    (SmAHTR) proposed by Green et al. (Green et al., 2010) is an example of a cross flow heat  
40    exchanger. The SmAHTR PHX utilizes a crossflow shell and tube heat configuration with the  
41    radioactive salt on the shell side (‘primary’) and the non-radioactive salt on the tube side  
42    (‘secondary’). The PHX is curved to fit along the pressure vessel walls. In order to design these  
43    heat exchangers accurately, data is needed for total pressure drop on both sides as well as heat  
44    transfer coefficients. Unfortunately, the correlations and data available for these quantities are  
45    limited to basic empirical correlations for pressure drop and heat transfer proposed by Zukauskas  
46    and Ulinskas (Zukauskas and Ulinskas, 1988) for air, water, and liquid metals in simple  
47    geometries. The pressure drop correlations are limited to adiabatic conditions which may not  
48    accurately account for the thermal effects on fluid properties. This lack of experimental data

presents a limitation when designing crossflow heat exchangers for MSRs. This can be addressed by both experimental and computational efforts.

In an effort to provide a starting point for future design and experimental work to remedy the lack of information, a computational fluid dynamics (CFD) campaign is being conducted. In order to start the analysis from a reasonably well-understood point, an in-line tube bank with FLiBe ( $\text{LiF-BeF}_2$ ), a frequently selected molten salt in MSRs, was selected for these simulations. The objective of this work is to define and evaluate a methodology for simulating overall flow behavior (i.e. total pressure drop) for use in design studies when more sophisticated methods such as LES or uRANS are unavailable.

## 2 Literature Survey:

Early experimental work on tube banks was to measure heat transfer around cylindrical tube heat exchangers was performed by Aiba, Tsuchida and Ota in the 1980s (Aiba et al., 1980). Heat transfer was measured for turbulent flows of air for both in-line and staggered tube banks (Aiba et al., 1982; Aiba and Hajime, 1982). Experiments for in-line tube banks covered a narrow range of Reynolds numbers,  $10^4 - 4 \times 10^4$ . For these conditions, they demonstrated that the Nusselt number for the first cylinder varied considerably with spacing. The Nusselt number on the remaining cylinders, however, showed little sensitivity to tube spacing. The authors also noticed a strong deflection of the flow for a uniform pitch to diameter ratio of 1.3.

In 2011, Afgan, Kahil, et al. performed simulations of flow around a single cylinder and two side-by-side cylinders using an LES turbulence model for a moderate Reynolds number,  $\sim 3000$  (Afgan et al., 2011). In the side-by-side simulations, they tested a range of pitch to diameter ratios. They found that for a pitch to diameter ratio of unity, the tubes acted as a single bluff body. In intermediate ranges, 1.25 – 1.75, they predicted an oscillatory flow pattern similar to that previously observed in experimental studies (Aiba et al., 1980). For higher gap ratios ( $>2.0$ ), the authors' results showed less interaction in the wakes, forming a flow pattern better characterized as two independent cylinders.

The ability of various turbulence models to predict pressure and heat transfer distributions over the surface of a tube in a periodic bundle was studied by Iacovides, Launder, et al. in 2013 (Iacovides et al., 2013). They simulated a flow using LES as well as various uRANS type turbulence models including the  $\kappa$ - $\omega$  SST (Menter) and  $\kappa$ - $\epsilon$  formulations. Their chosen case for the uRANS simulations was a 2x2 bank domain with a pitch to diameter ratio of 1.6 at a Reynolds number of 41,000. This was chosen to “pose a challenge” as this ratio seems to be on the threshold for a deviated flow direction. The presented LES results demonstrated clear evidence of the flow deflecting from a straight-through path. This was failed to be accurately reproduced by any of the uRANS simulations.

More recently, Bae, Kim, and Kim used an LES method to simulate flows around a 2x10 tube bundle (Bae et al., 2015). Interestingly, for uniformly distributed tubes at a pitch to diameter ratio of 1.5, they did not predict that the flow would be deflected. However, their simulations were run for a much lower Reynolds number of 6300. They did observe the formation of asymmetric vortex pairs behind the tubes, which may indicate an oscillatory flow pattern was developing.

1  
2  
3  
4 It is clear from the surveyed literature that crossflows in tube bundles produces a complex flow  
5 pattern. Comparatively few studies have been conducted for low pitch-to-diameter ratios (<1.3)  
6 where the interaction between wakes behind cylinders becomes more significant and practically  
7 none have attempted to evaluate the applicability of steady RANS methods. It is expected that  
8 steady RANS will be unable to properly resolve the flow phenomena and cannot be relied on to  
9 provide high-accuracy evaluations of design parameters. However, it is likely that a RANS  
10 method can provide accurate enough simulations to inform scoping calculations, useful in  
11 narrowing the scope of a more in-depth analysis.  
12  
13

14  
15 **3 Numerical Approach:**  
16  
17

18 The CFD simulations were performed using CD-Adapco's Star-CCM+ v10.04.011 (CD-Adapco,  
19 2020). The following subsections outline the geometry, meshing, and simulation set up.

21  
22 **3.1 Geometry and Meshing**  
23

24 The bundle geometry investigated for this study was partially based on of the SmAHTR (Green et  
25 al., 2010) PHX found in Figure 1. However, while the SmAHTR design uses a curved geometry  
26 and a staggered tube arrangement, the studied geometry uses a straight geometry with an in-line  
27 tube arrangement. These geometric changes were chosen to simplify the analysis and isolate  
28 sensitivities while retaining the interesting flow phenomena. The reference tube bank is presented  
29 in Figure 2 using the physical dimensions found in Table 1. The subdomains (referred to as flow  
30 channels) shown in Figure 2 on the right are examples of the 1 and 5 flow channels used for this  
31 study. Plenums were added at the inlet and outlet of the simulation domain to prevent the  
32 development of backflow. Backflow at these boundaries contributed to convergence issues for the  
33 simulations.  
34  
35

36  
37  
38  
39  
40  
41  
42  
43  
44  
45  
46  
47  
48  
49  
50  
51  
52  
53  
54  
55  
56  
57  
58  
59  
60  
61  
62  
63  
64  
65

What eqns are you solving for?  
Single or multiphase?

1  
2  
3  
4  
5  
6  
7  
8  
9  
10  
11  
12  
13  
14  
15  
16  
17  
18  
19  
20  
21  
22  
23  
24  
25  
26  
27  
28  
29  
30  
31

ORNL 2011-G00132/chj

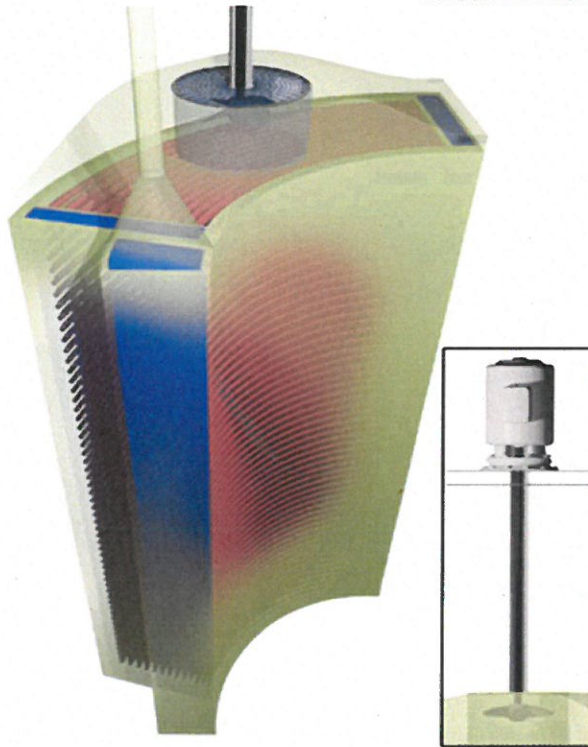


Figure 1 - SmAHTR Primary Heat Exchanger (Green et al., 2010)

The meshes were created using the built-in Star-CCM+ meshing tool for each flow domain. The trim mesher was used to mesh the mean flow region while the prism layer mesher was used to mesh the near wall region. The trimmer mesher is a hexahedral mesher that trims cells near wall/surface regions. The near wall/surface regions are meshed using the prism layer mesher to build cells on the surfaces to capture the boundary layer of the flow. The inlet and outlet plenums were created by extruding the inlet and outlet surface meshes out to a distance of 0.0762 m. In addition, a mesh sensitivity study was performed and is presented in section 4.1.

mesh resolution ?

44  
45  
46  
47  
48  
49  
50  
51  
52  
53  
54  
55  
56  
57  
58  
59  
60  
61  
62  
63  
64  
65

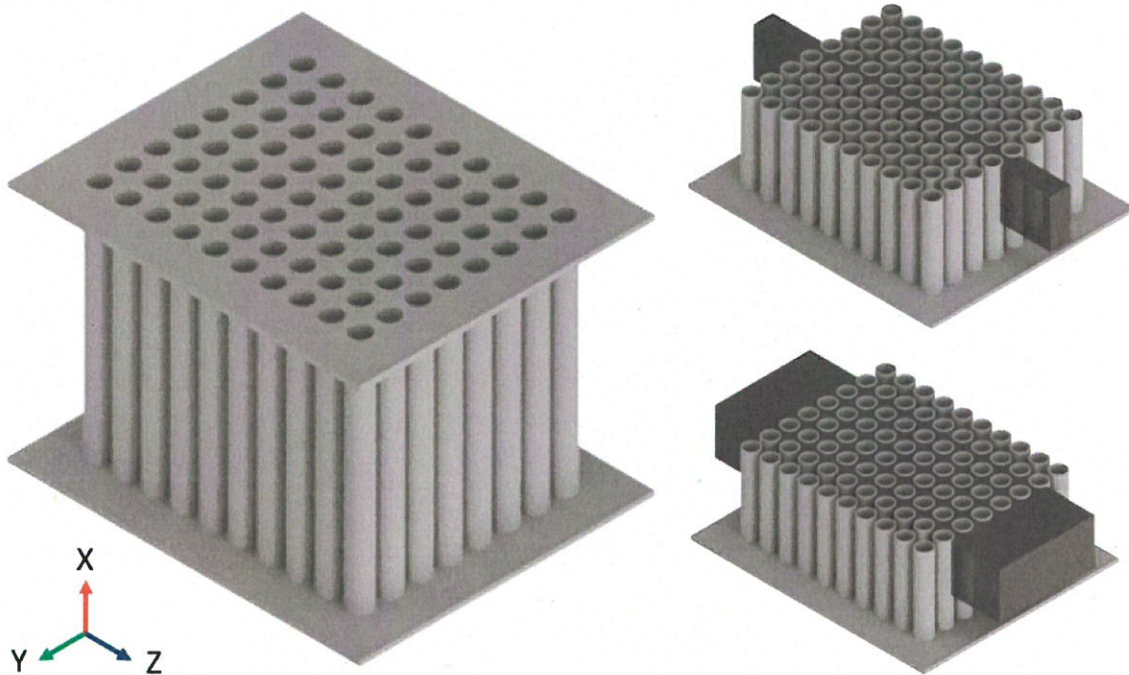


Figure 2 – Tube Bundle (Left) and Internal Fluid Domains - 1-FC – Top Right and 5-FC – Bottom Right

Table 1 - Geometric Properties of the Tube Bundle

Property	Value
Tube Diameter	2.54 cm
Bundle Arrangement	Inline (Square)
Pitch to Diameter Ratio – Transversal	1.25
Pitch to Diameter Ratio – Longitudinal (Stream wise)	1.25
Height	2.54 cm

### 3.2 Modeling Setup

The boundary conditions for the simulations were selected to reduce the computational effort and to focus on “central” behavior (i.e. with no effect from heat exchanger walls). The boundaries normal to the vertical direction (x-direction, span-wise) were set as periodic boundaries without any forcing functions. The boundaries normal to the y-direction (transverse) were also set to periodic boundaries without any forcing functions for most of the presented simulations. The periodic boundary conditions were compared to symmetric boundary conditions in the transverse direction for one flow channel in section 4.2. The inlet boundary is a uniform (flat) velocity set to 0.5 m/s which corresponds to a Reynolds number of ~22000. The Reynolds number was based on

max velocity in minimum area between tubes and tube diameter as the characteristic length scale. The tube walls were treated as standard non-slip wall boundaries. The boundary conditions are summarized in Table 2 and a diagram with the pertinent boundary conditions is shown in Fig. 3. The direction of the mean flow is perpendicular to the tube bank in alignment with the stream wise direction.

Values for the density ( $1940 \text{ kg/m}^3$ ) and dynamic viscosity ( $0.0056 \text{ kg/m}\cdot\text{s}$ ) of FLiBe salt used in this study were obtained from Sohal et al. (Sohal et al., 2010) and Forsberg et al. (Forsberg and Renault, 2007) at a pressure of 1 atm and a temperature of  $700^\circ\text{C}$ .

Table 2 – Boundary Conditions for Simulations

Number	Boundary Type	Value	Color
1	Velocity Inlet	0.5 m/s	Red
2	Y Axis (Transverse) - Periodic/Symmetry	-	Black
3	Pressure Outlet	0 Pa	Blue
-	X Axis (Vertical) - Periodic	-	Not Shown
-	Walls - Non-Slip	-	-

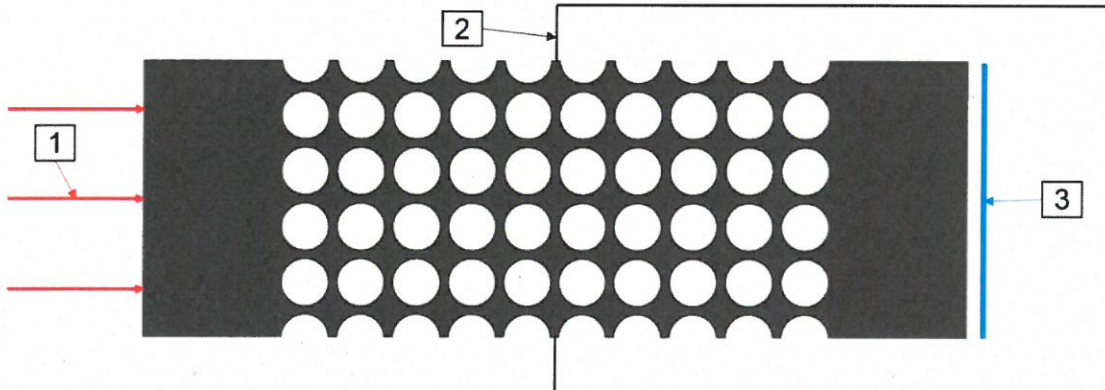


Figure 3 - Graphical Representation of Boundary Conditions

### 3.3 Modeling Framework

A Reynolds-Averaged Navier-Stokes (RANS) framework and the finite volume method was used in Star CCM+ for all simulations. Turbulence was modeled using various one- and two-equation models and the results were compared as a focus of this study (see section 4.4). The convergence criteria were defined as the reduction of x, y, and z momentum and continuity residuals by at least 3 orders of magnitude. Additionally, the pressure drop, centerline velocity magnitude and pressure fields were monitored between iterations to ensure convergence.

1  
2  
3  
4     3.3.1 Turbulence Models  
5  
6

7     9 The different turbulence models investigated were chosen based on their relative popularity and  
8 widespread use in industry. They were evaluated for their ability to reasonably predict the flow  
9 behavior of interest in this work. A few types of turbulence model families were selected based on  
10 previous usage in tube bundle crossflow and separated flows (Beladjine et al., 2015; Iacovides et  
11 al., 2013). The selection of turbulence models in the steady RANS framework was motivated by  
12 previous efforts of Iacovides et al. (Iacovides et al., 2013) and Beladjine et al. (Beladjine et al.,  
13 2015) focused on unsteady RANS simulations. Though, the usage of these turbulence models for  
14 steady simulations can be difficult due to the inherent complexity of the underlying flow  
15 phenomena.  
16

17  
18     The  $\kappa-\epsilon$  turbulence models selected were the standard low Re  $\kappa-\epsilon$  and the realizable  $\kappa-\epsilon$  variants.  
19 The standard low Re  $\kappa-\epsilon$  is selected due to its high usage in research and industry. It does have  
20 notable deficiencies such as in separated flows on curved surfaces. The realizable  $\kappa-\epsilon$  model was  
21 formulated to overcome some of these deficiencies. Of particular interest are the improved  
22 predictions for flows experiencing separation and rotation as flow separation is expected to be  
23 significant in tube bundles.  
24

25  
26     The  $\kappa-\omega$  SST (Menter) and Spalart-Allmaras (SA) turbulence models were selected due to their  
27 purported ability to more accurately simulate flow separation compared to the  $\kappa-\epsilon$  model. The SA  
28 turbulence model is of particular interest as it is only a one equation model as opposed to  $\kappa-\epsilon$  or  $\kappa-\omega$   
29 families, which solve two scalar transport equations. The  $\kappa-\omega$  SST is generally considered to  
30 produce reasonable predictions within separated flows and solves the kinetic energy and specific  
31 dissipation equations.  
32

33  
34     All models were run with the “all- $y^+$ ” wall treatment formulation which is a blend of using wall  
35 functions for high  $y^+$  values and resolving the flow all the way to the wall. Although, particular  
36 care was taken to keep the  $y^+$  close to 1 for near wall mesh cells.  
37

38     4     Results and Discussions:  
39  
40

41     4.1 Mesh Independence Study  
42  
43

44  
45     The mesh independence study was conducted using the standard low Re  $\kappa-\epsilon$  turbulence model for  
46 the 1-flow channel domain with periodic boundaries in both the transverse and vertical directions.  
47 Four different mesh sizes were tested, they were varied by reducing the base cell size and  
48 maximum allowed size by half for each reduction. This enabled a significant increase in mesh  
49 density for each successive mesh while maintaining a constant refinement strategy. Mesh M1  
50 represents the coarsest mesh and mesh M4 represents the finest. The pressure drop between the  
51 inlet and outlet as well as line plots of the velocity and pressure along the centerline of the tube  
52 banks were compared as criteria for mesh convergence.  
53

54  
55     The usage of the grid convergence index (GCI) developed by Roache (Roache, 1994) for the  
56 pressure drop parameter was attempted for this study. Oscillatory convergence of pressure drop  
57

Reasoning for choosing such  
entirely diff Turb submodels?

1  
2  
3  
4  
5  
6  
7  
8  
9  
10  
11  
12  
13  
14  
15  
16  
17  
18  
19  
20  
21  
22  
23  
24  
25  
26  
27  
28  
29  
30  
31  
32  
33  
34  
35  
36  
37  
38  
39  
40  
41  
42  
43  
44  
45  
46  
47  
48  
49  
50  
51  
52  
53  
54  
55  
56  
57  
58  
59  
60  
61  
62  
63  
64  
65

was encountered which prevents proper implementation of GCI, requiring a different approach to be used. In order to determine mesh convergence based on the pressure drop, two metrics were adopted: comparison to a correlation and comparison to the finest mesh. These provide reasonable comparisons to determine what constitutes a “converged” solution. The empirical correlation proposed by Zukauskas and Ulinskas (Zukauskas and Ulinskas, 1988) for predicting pressure drops in crossflow tube bundles was used for the first metric. The predicted pressure drops are shown in Table 3 along with the corresponding comparisons as percent difference.

Table 3 - Comparison of Pressure Drops of Different Meshes and Empirical Correlation

Prediction	Pressure drop (kPa)	Percent error (compared to ?)	Percent difference (compared to M4)
M1	21.35	-2.69	11.57
M2	23.36	6.47	2.58
M3	22.94	4.56	4.43
M4	23.97	9.25	--
ZU-Empirical	21.94	--	--

The pressure drops for each successive mesh oscillate around one value, which exemplifies the previously stated issue with using GCI. All of the predictions were within a reasonable +/- 10% error from the empirical prediction, where the M1 and M3 meshes had the lowest differences.

The percent difference calculations for the different meshes compared to the finest mesh (M4) show a significant reduction from mesh M1 to mesh M2, but only a marginal difference was observed with further mesh refinement between mesh M2 and mesh M3. This indicates the flow behavior is not well resolved with the M1 mesh whereas the M2 and M3 meshes predict the pressure drop within 5% difference of the prediction using mesh M4.

In order to take a deeper look at the flow behavior, the velocity and pressure distributions are provided in Figure 4 and Figure 5. The velocity is non-dimensionalized using the average velocity ( $V_f$ ) defined at the inlet of the domain. The pressure is non-dimensionalized using the dynamic pressure at the inlet of the domain using the same inlet average velocity.

And how can one guarantee that the M4 is ~~refined enough~~? sufficiently refined?  
What are the mesh resolutions?

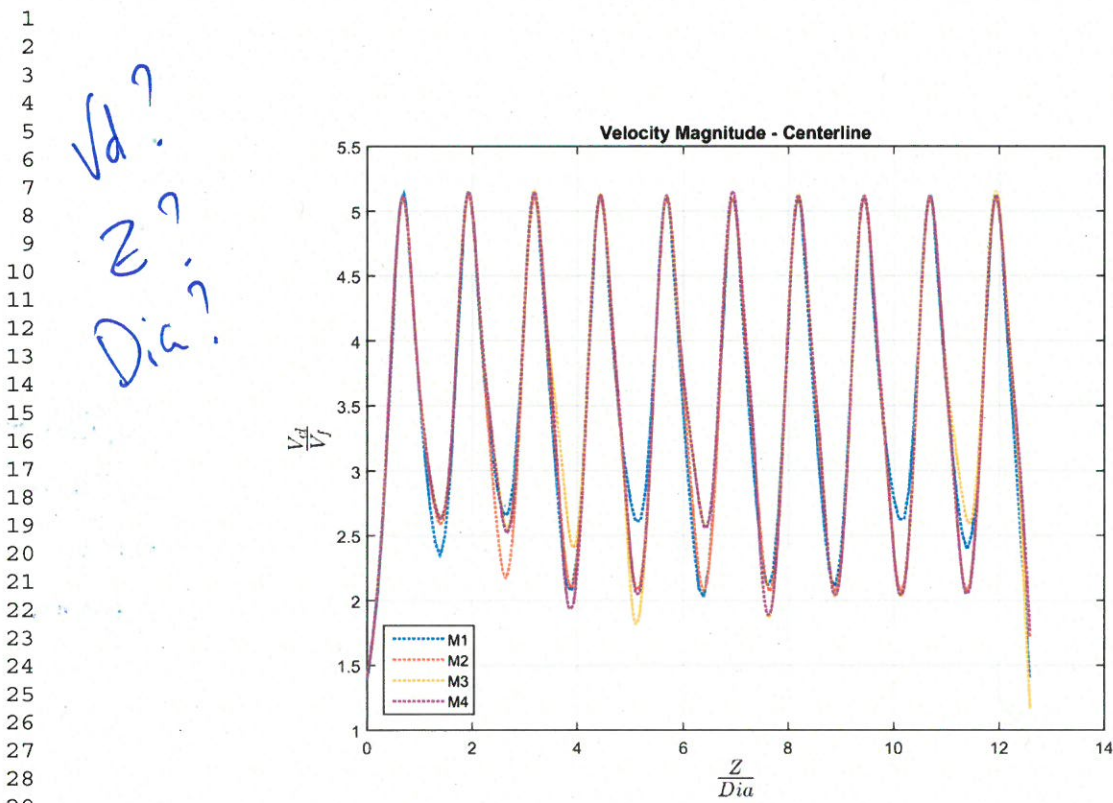


Figure 4 - Centerline Velocity Magnitude along Stream wise Direction

The velocity profiles are observed to oscillate between maximum and minimum values corresponding to the reductions and expansions of flow area associated with the gaps between tubes. The different minimum velocities in the different gaps indicate flow separation and reattachment occurs between each row of tubes. The behavior shows approximately the same trends for all four meshes which make qualitative comparisons difficult. The slightly larger number of deviations of the M1 does indicate some features are not being resolved.



P  
l  
y  
?

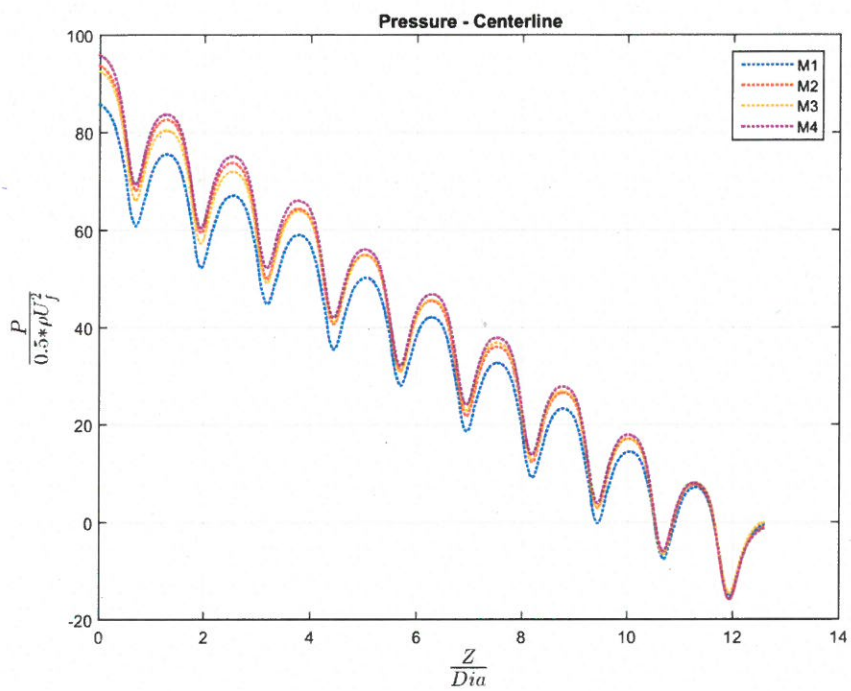


Figure 5 – Centerline Pressure along Stream Wise Direction

The four pressure predictions along the centerline axis are observed to have similar behavior. The M1 mesh provides the only notable deviation that serves as additional evidence that it would not be sufficient for further studies. Otherwise, M2, M3, and M4 predictions show only minor differences.

Based on the comparisons of the pressure drops of the different meshes, the M3 mesh provided the most balanced trade-off in terms of prediction and computational cost. The velocity prediction along the centerline of M3 was observed to have the fewest deviations from M4 and the pressure predictions were not observed to have significant differences. Additionally, the computational demands of the M3 mesh allows for the later studies to occur within a reasonable amount of time. This encouraged the selection of the M3 mesh for the further studies in this work.

#### 4.2 Boundary Condition Study

It is expected that a symmetry boundary condition in the transverse direction would restrict the flow domain by removing a degree of freedom for the fluid motion, i.e. around the cylindrical tubes. This would certainly be most pronounced when using only a single flow channel. However, it is useful to understand what effect this would have on the predicted overall pressure drop. Additionally, adding flow channels to the domain would mitigate the effect of the symmetry boundary condition, eventually reaching the point where the differences between a symmetry, periodic, or even solid wall boundary condition would be minimal. Since the interest of the current work lies in determining the overall effect of the symmetry boundary condition, the boundary

1  
2  
3  
4 condition study is limited to only a single channel domain, in which the boundary condition is  
5 expected to have the greatest effect.  
6

7  
8 The boundary condition study was conducted utilizing 1 flow channel domain and the M3 mesh  
9 with varying boundary conditions in the transverse direction. The boundary condition in the  
10 vertical direction was unchanged as the flow exhibits 2D behavior, which is practically invariant  
11 in the vertical direction. The pressure drops, as well as velocity and pressure distributions are  
12 provided for analysis of the most appropriate conditions for the given P/D ratio and initial  
13 conditions.  
14

15  
16 The pressure drops for each boundary condition set are compared to the Zukauskas prediction for  
17 the same flow conditions in Table 4. The SYM prediction has a large observable difference from  
18 both the Zukauskas and PER predictions. The use of the SYM boundary condition causes the  
19 simulation to predict a pressure drop significantly lower than both the correlation value as well as  
20 the value predicted using PER boundaries. This motivates investigating the behavior of the flow  
21 inside the flow channel.  
22

23  
24  
25 Table 4 - Boundary Condition Study Pressure Predictions  
26  
27  
28

Boundary Condition	Pressure Difference (kPa)	Percent error (compared to ZU)
PER	22.9	4.52
SYM	16.5	-24.72
ZU-Empirical	21.9	--

35  
36 The smoothed velocity contours for both the PER and SYM simulations on the XZ plane are  
37 presented in Figure 6. The PER simulation presents flow deflection in the transverse direction  
38 where the flow has separated in either the positive or negative directions. The favoring of the flow  
39 in either direction occurs seemingly at random, the cause of which cannot be determined using this  
40 method and is likely beyond the capability of the steady RANS framework. The occurrence of the  
41 flow separation is due to the low resistance to crossflow in either direction. The simulation using  
42 the SYM boundary is observed to have no flow separation or reattachment occur along the tube  
43 walls. The fluid flows directly between the rows due to the large resistance to crossflow from the  
44 symmetry boundary conditions. The complexity of the path taken by the flow in the PER  
45 simulation is likely why the pressure drop is much closer to the prediction from the Zukauskas  
46 correlation.  
47

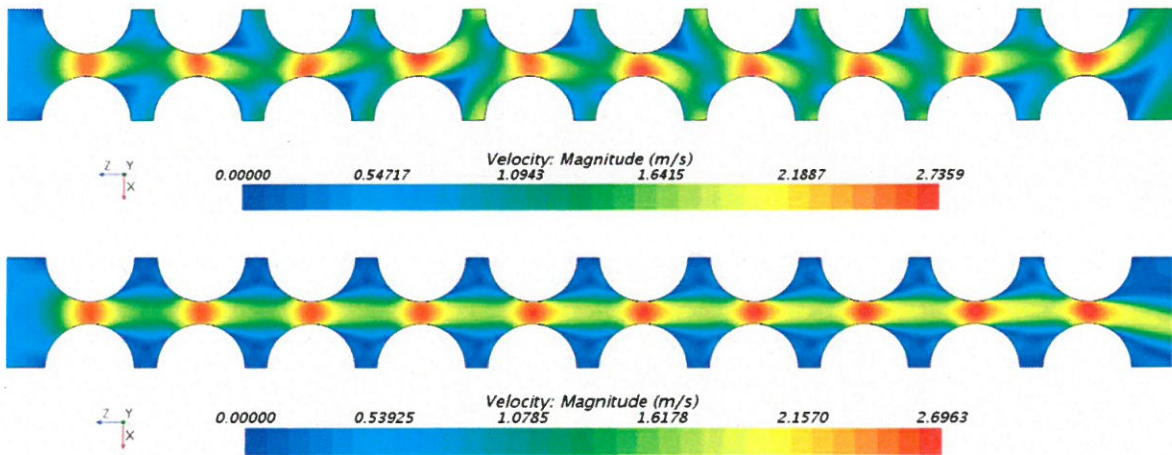


Figure 6 - Velocity Contours for the Periodic (Top) and Symmetry (Bottom) Simulations

The velocity and pressure profiles along the centerline of the stream wise direction are provided in Figures 7 and 8. The PER and SYM velocity predictions are observed to have significant magnitude differences in expanded regions between the rows of tubes. The lower velocity seen for the PER simulations correspond to the flow attachment and separation on the tube walls. The smaller drops in velocity magnitude for the SYM simulation parallels the behavior seen in Figure 6. The drop in velocity is not from the flow instabilities but from the domain expansion between the rows.

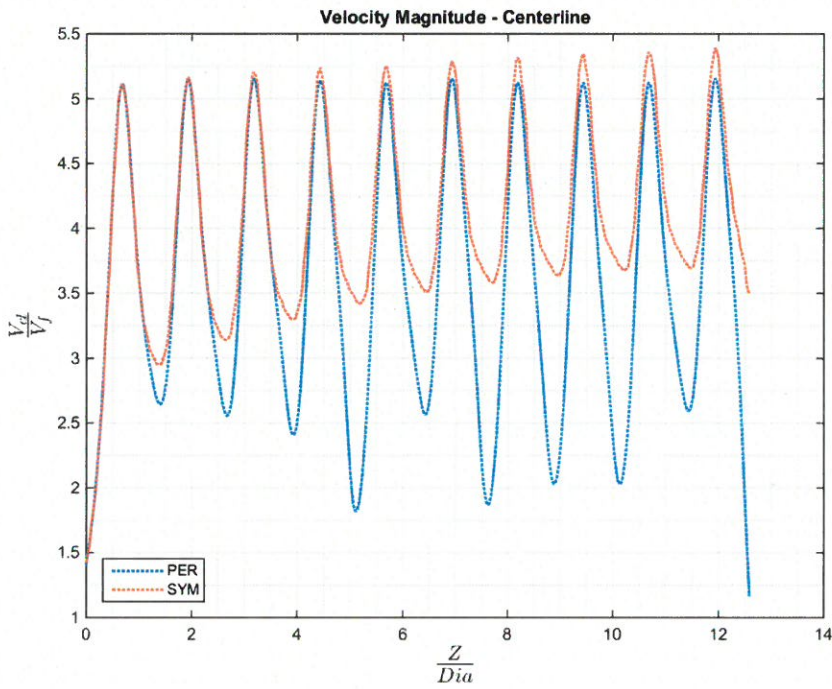


Figure 7 - Centerline Velocity Magnitude along Stream Wise Direction for Different Transverse Boundary Conditions

The pressure predictions between the SYM and PER simulations have similar trends with significantly different magnitudes. The SYM prediction does have “forward” peaking of the “bells” of the pressure which occur in between the rows. The forward peaking corresponds with increasing higher maximum velocity in the higher velocity regions. This further exemplifies the higher resistance to crossflow seen in the SYM vs. PER simulations.

The under prediction of the pressure drop of the symmetric boundaries to the Zukauskas and periodic boundaries suggests that type of boundary condition is not appropriate for these simulations, as was expected. The artificially high resistance to crossflow eliminates the irregular flow behavior (deflection) that is expected for a tube bundle of this pitch to diameter ratio for this Reynolds number. As such, further studies are conducted with periodic conditions for a more accurate representation of the flow behavior and pressure drops.

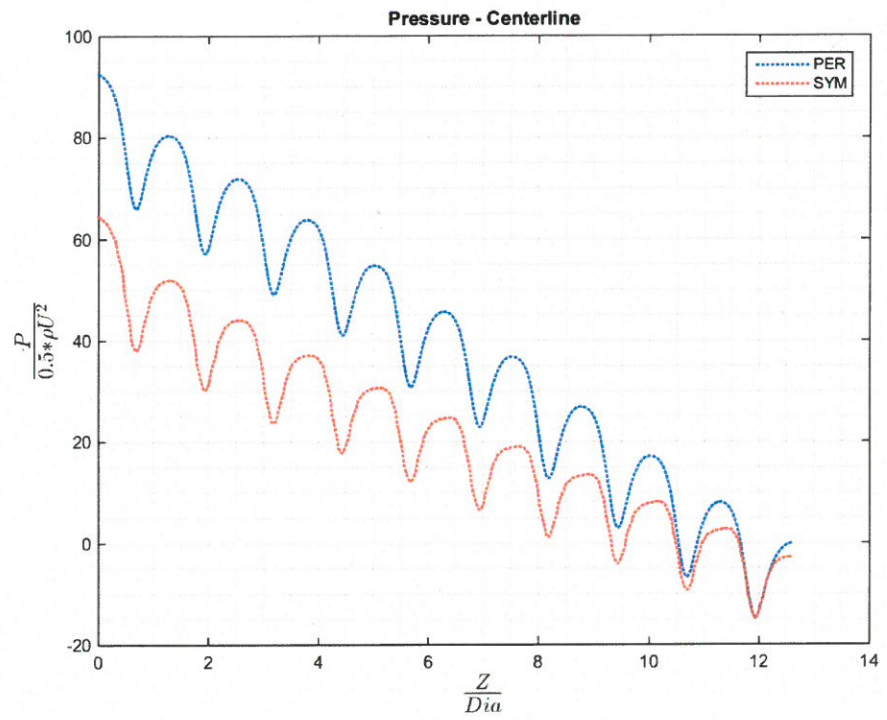


Figure 8 - Centerline Pressure along Stream Wise Direction for Different Transverse Boundary Conditions

### 4.3 Flow Domain Study

The flow domain was studied using the previously documented initial and boundary conditions, meshing parameters, and standard low Re  $\kappa$ - $\epsilon$  turbulence model. The sensitivity of the size of the domain was investigated due to the potential effect on the resulting pressure and flow behavior. The domain size was increased by adding additional flow channels in the transverse direction until reaching five flow channels. Only up to five flow channels were investigated due to computational limitations past this number.

The pressure drops for each domain are compared to the Zukauskas prediction with percent error reported in Table 5. The pressure drops were found to be insensitive enlarging the domain size due to the low variation of the predictions, (1-2 kPa). The low variation is expected as the resistance presented to the flow does not substantially vary between domain sizes. The size of the domain (number of flow channels) for pressure drop is not considered to be greatly important within the steady RANS framework.

Table 5 – Flow Domain Study Pressure Drop Comparisons

<b>Flow Channel</b>	<b>Pressure Difference (kPa)</b>	<b>Percent error (compared to ZU)</b>
1	22.9	4.52
2	23.5	7.24
3	22.5	2.63
4	23.5	7.83
5	24.3	10.82
ZU-Empirical	21.9	-

The centerline velocity magnitudes of each domain within the most representative flow channel are shown in Figure 9 and Figure 10. The single flow channel was observed to be qualitatively different for the majority of maximum and minimum regions. Otherwise, the non-convergence of behavior of increasing flow channels indicates that the number of required flow channels cannot be determined using a steady RANS framework. From these observations, at least two or three flow channels should be adequate to investigate pressure drop or to obtain a qualitative description of the flow. One flow channel could be used with conservatism if computational resources are particularly limited.

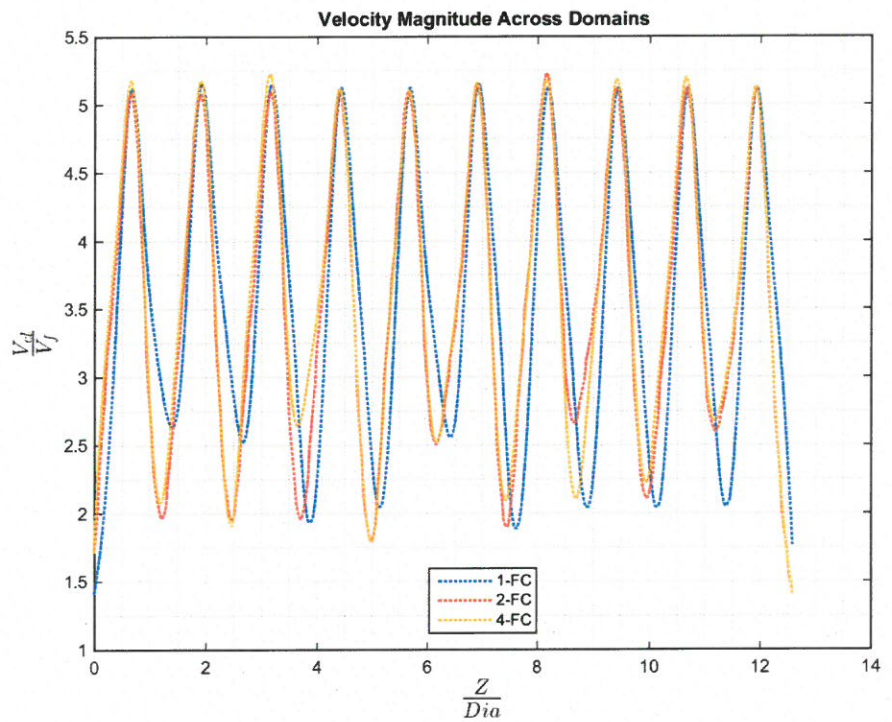


Figure 9 - Centerline Velocity Magnitudes along Stream Wise Direction for Different Domain Sizes – Even

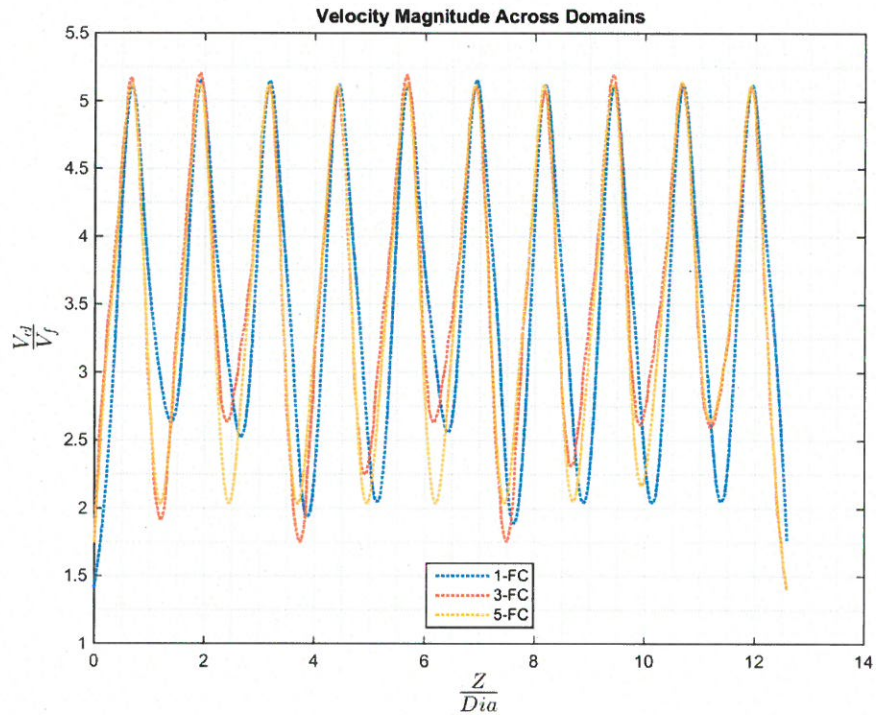


Figure 10- Centerline Velocity Magnitudes along Stream Wise Direction for Different Domain Sizes – Odd

#### 4.4 Turbulence Model Study

The appropriateness of a suitable turbulence model to be used for determining the desired parameters is important to address in this geometry. In this study, the focus is solely on usage of a steady framework which limits the application of several turbulence models. This is due to the issues of the inherent instabilities in the flow which cause convergence problems for some turbulence models. The instabilities are evident in the form of flow deflection in the wakes that are observed in Figure 11.

Can you BS now  
specific?

1  
2  
3  
4  
5  
6  
7  
8  
9  
10  
11  
12  
13  
14  
15  
16  
17  
18  
19  
20  
21  
22  
23  
24  
25  
26  
27  
28  
29  
30  
31  
32  
33  
34  
35  
36  
37  
38  
39  
40  
41  
42  
43  
44  
45  
46  
47  
48  
49  
50  
51  
52  
53  
54  
55  
56  
57  
58  
59  
60  
61  
62  
63  
64  
65

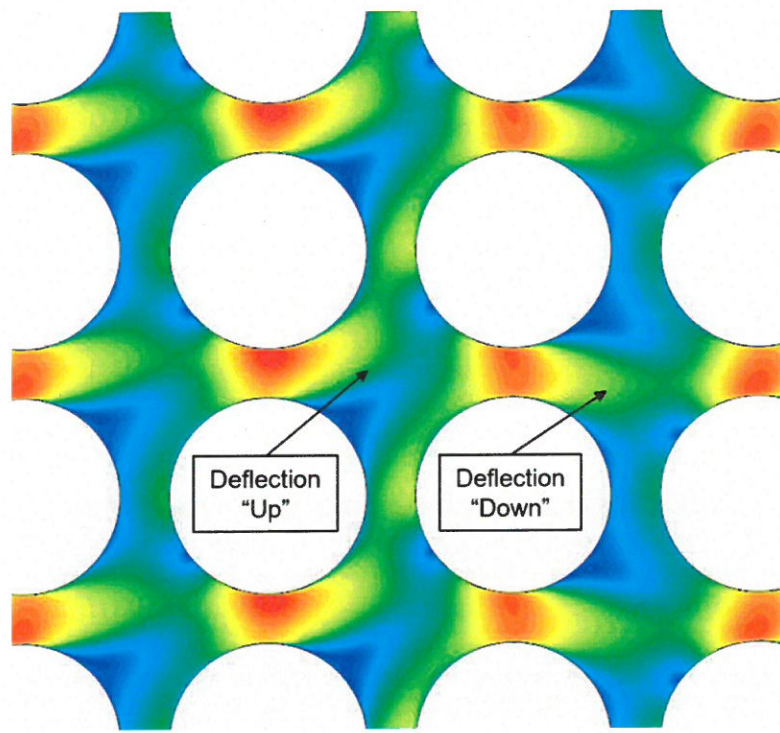


Figure 11 – Flow Deflection in the Crossflow Tube Bank

From this study, it was found that the standard low  $Re$   $\kappa-\epsilon$  (Lien) turbulence has very good convergence as compared the other turbulence models. The SA,  $\kappa-\omega$  SST, and Realizable  $\kappa-\epsilon$  turbulence models experienced issues with convergence and in some cases over predicted the pressure drop (Table 6). SA provided a reasonable prediction, but did not properly converge. This provides a dubious option for predicting pressure drop using this model. By explicitly, not resolving the deflection features, a suitable prediction of pressure drop can be determined in a steady framework.

Table 6 - Pressure Drops for Turbulence Model Study

Turbulence Model	Pressure Difference (kPa)	Percent error (compared to ZU)
Low Re $k-e$	22.5	2.6
Realizable $k-e$	24.5	11.5
Shear Stress Transport	27.9	27.1
SA	23.2	5.8
ZU-Empirical	21.9	--

## 5 Conclusions:

The studies provides a steady RANS methodology to model crossflow behavior of isothermal molten salts in a compact in-line tube bank. The previous methodologies use higher fidelity

1  
2  
3  
4 frameworks such as unsteady RANS and LES which require significant computational resources.  
5 The studies look at the feasibility of applying steady RANS and where possible pitfalls of the  
6 framework can occur. The resulting analysis determined that basic pressure drops were able to be  
7 predicted with reasonable accuracy. The strength of the predictions were based on a correlation  
8 previously developed from available experimental data sets created for fluids other than molten  
9 salts.  
10

11  
12 The boundary conditions in the transverse direction were investigated for sensitivity to periodic or  
13 symmetric boundary conditions. The periodic boundary condition was found to be more  
14 appropriate due to artificially high resistance to lateral flow presented by use of symmetric  
15 boundary conditions in the transverse direction. This was found by the significantly lower  
16 predicted pressure drop of the symmetric boundary conditions. Further, the artificially high  
17 resistance to crossflow was observed from both velocity and pressure distributions in the domain.  
18  
19

20  
21 The size of the flow domain was investigated by increasing the number of flow channels from one  
22 to five channels in the transverse direction. The predictive capabilities for pressure drop was found  
23 to be reasonable with increasing the size of the flow domain. The velocity distribution along the  
24 length of the domain was found to be qualitatively different between the single flow channel and  
25 multiple flow channels. The usage of two or more flow channels is encouraged due to only minor  
26 quantitative differences between increasing the number of flow channels more than two.  
27  
28

29 A feasibility of turbulence model study was conducted to investigate the applicability of turbulence  
30 models used for unsteady RANS simulations of similar work. The turbulence models investigated  
31 were the standard low Re  $\kappa-\epsilon$  (Lien), Realizable  $\kappa-\epsilon$ , Spalart-Allmaras, and the  $\kappa-\omega$  SST (Menter)  
32 turbulence models. The standard low Re  $\kappa-\epsilon$  (Lien) turbulence model was determined to provide a  
33 reasonable prediction of pressure drop within the desired convergence criteria. This is likely due  
34 to the behavior it is explicitly not resolving.  
35  
36

37 The provided methodology can be used to determine predictions of pressure drops within an  
38 isothermal tube bank in a crossflow arrangement for simplified analysis. This can help provide  
39 reasonable starting points for crossflow heat exchanger designs involving compact arrangement of  
40 an in-line tube bank.  
41  
42

## 43     6 Acknowledgements:

44  
45 This material is based upon work supported under a Department of Energy, Office of Nuclear  
46 Energy Integrated University Programs Graduate Fellowship.  
47  
48

49 Portions of this research were conducted with high performance research computing resources  
50 provided by Texas A&M University (<http://hprc.tamu.edu>).  
51  
52

## 53     7 References:

- 54  
55  
56 Afgan, I., Kahil, Y., Benhamadouche, S., Sagaut, P., 2011. Large eddy simulation of the flow  
57 around single and two side-by-side cylinders at subcritical Reynolds numbers. Phys. Fluids  
58 23, 1–17. doi:10.1063/1.3596267  
59  
60 Aiba, S., Hajime, T., 1982. Heat Transfer Around Tubes in Inline Tube Banks. Bull. JSME 25,  
61  
62  
63  
64  
65

- 1  
2  
3  
4 919–924.  
5 Aiba, S., Tsuchida, H., Ota, T., 1980. Heat Transfer Around a Tube in a Bank. Bull. JSME 23, 1163–1170. doi:10.1248/cpb.37.3229  
6  
7 Aiba, S., Tsuchida, H., Terukazu, O., 1982. Heat Transfer around Tubes in Staggered Tube  
8 Banks. Bull. JSME 25, 927–933.  
9  
10 Bae, Y., Kim, Y.I., Kim, K.K., 2015. Computation of Turbulent Cross-Flow Over an in-Line  
11 Tube Bundle, in: Proceedings of the 9th International Symposium on Turbulence and Shear  
12 Flow Phenomena (TSFP-9). TSFP-9, Melbourne, Australia, pp. 1–6.  
13 Beladjine, B., Aounallah, M., Belkadi, M., Aadjlout, L., Imine, O., 2015. On the use of the  
14 periodicity condition in cross-flow tube, in: EPJ Web of Conferences. EPJ Web of  
15 Conferences, pp. 1–7. doi:10.1051/epjconf/20159202005  
16 CD-Adapco, 2016. Star-CCM+ 10.06.010 User's Guide.  
17 Forsberg, C.W., Renault, C., 2007. Liquid Salt Applications and Molten Salt Reactors. Proc.  
18 ICAPP'07 1–13.  
19 Green, S.R., Gehin, J.C., Holcomb, D.E., Carbajo, J.J., Ilas, D., Cisneros, a T., Varma, V.K.,  
20 Wilson, D.F., Jr, G.L.Y., Peretz, F.J., Bradley, E.C., Bell, G.L., Hunn, J.D., 2010. Pre-  
21 Conceptual Design of a Fluoride- Salt-Cooled Small Modular Advanced High-Temperature  
22 Reactor (SmAHTR).  
23 Iacovides, H., Launder, B., Laurence, D., West, A., 2013. Alternative Strategies for Modelling  
24 Flow over In-Line Tube Banks, in: Proceedings of the 8th International Symposium on  
25 Turbulence and Shear Flow Phenomena (TSFP-8). Begel House Inc., Poitiers, France, pp.  
26 1–6.  
27 Roache, P.J., 1994. Perspective: A method for uniform reporting of grid refinement studies. J.  
28 Fluids Eng. 116, 405–413.  
29 Sabharwall, P., Collins, J., Clark, D., Siahpush, A., Phoenix, W., Mckellar, M., Patterson, M.,  
30 2012. Technology Development Roadmap for the Advanced High Temperature Reactor  
31 Secondary Heat Exchanger. doi:INL/EXT-12/26219  
32 Sohal, M.S., Ebner, M. a, Sabharwall, P., Sharpe, P., 2010. Engineering database of liquid salt  
33 thermophysical and thermochemical properties. Idaho Natl. Lab. Idaho Falls CrossRef 1–  
34 70. doi:ext-10-18297  
35 Zukauskas, A., Ulinskas, R., 1988. Heat transfer in tube banks in crossflow, Experimental and  
36 applied heat transfer guide books. Hemisphere Pub. Corp., New York.  
37  
38  
39  
40  
41  
42  
43  
44  
45  
46  
47  
48  
49  
50  
51  
52  
53  
54  
55  
56  
57  
58  
59  
60  
61  
62  
63  
64  
65

**Figure**



Figure 1 - SmAHTR Primary Heat Exchanger (Green et al., 2010)